Searching Chimera States in the Nonlocal Complex Ginzburg Landau Equation

AUTHOR: Pedro Parrado Rodríguez

Master Thesis

Master's degree in Physics of Complex Systems
at the
UNIVERSITAT DE LES ILLES BALEARS

Academic year 2015-2016

July 14, 2017

UIB Master's Thesis Supervisor: Damià Gomila

UIB Master's Thesis Co-Supervisor: Manuel Matias

Abstract

In this work, we will study the existence of chimera states in the Complex Ginzburg-Landau (CGL) equation with a non-local interaction. We have studied analytically the stability of the plane wave solutions of the equation (coherent states) and, using that result and numerical simulations, we find that the transition between the turbulent phase (incoherence) and the plane wave phase (coherence) is supercritical. Therefore, chimeras, as states in which coherent and incoherent states coexist, can not form in the CGL with these conditions.

We have also changed the kernel of the interaction to a general kernel using a moment expansion. However, this has proved insufficient to produce the conditions for the existence of the chimeras. Further research can be made by adding other nonlinear terms to the CGL equation in order to generate the appropiate conditions to observe a coexisting region in parameter space between coherent and incoherent states.

Contents

Chapter 1

Introduction

Recently, chimera states have become a field of increasing relevance. Scientists are finding these states in a lot of different systems, from systems of oscillators [3, 8] to networks of neurons [7]. The possible importance of chimera states ranges across various disciplines, pertaining to phenomena such as the unihemispheric sleep of animals, signal propagation through synchronized firing in otherwise chaotic neuronal networks, and the existence of turbulent-laminar patterns in Couette flow.

There are many studies about chimeras in different discrete models, and some of them have also been demonstrated in experiments. Nevertheless, the study of chimera states in continuous systems has received much less attention.
The most relevant example of chimera states in a continuous system has been found in a variation of the Complex Ginzburg-Landau (CGL) equation, using a non-local coupling. The model was proposed in a paper by Kuramoto and Battogtokh [6] and has become one of the most popular examples of chimera states. However, after a further analysis, we have found that these chimera states have been discovered in a system that does not represent properly a continuous system. Therefore, they can be only a spurious result product of an incorrect simulation.

The goal of this work is to make a proper analysis of the chimeras in the non local CGLE, and study their existence in proper simulations. In the following sections, we will introduce briefly the CGL equation and the chimera states. After that, we will deepen in the problem, and show the results of our numerical and analytical work. Finally, we will make different variations to the CGL equation, trying to find a condition that leads to the appearance of chimera states in a continuous system.

1.1 Complex Ginzburg-Landau equation

The complex Ginzburg-Landau equation is one of the most studied nonlinear equations in the physics community, and constitutes a generic model for extended systems at the onset of oscillations. It is important because it arises as the natural description of many physical situations, in particular of any oscillatory extended system close to a Hopf bifurcation. Its solutions display a very rich variety of dynamical behaviors when its parameters are changed, reflecting the interplay of dissipation, dispersion and nonlinearity.

Due to its generality, it is capable of describing many phenomena like spatio-temporal chaos in reaction-diffusion systems, nonlinear waves, second-order phase transitions, superconductivity or superfluidity [2].

The general form of the local CGL equation is given by:

$$\frac{\partial A}{\partial t} = A + (1 + ib)\Delta A - (1 + ic)|A|^2 A, \tag{1.1}$$

where A is a complex function of (scaled) time t and space $\vec{x}$ (often in reduced dimensions $D = 1$ or 2) and the real parameters b and c characterize linear and nonlinear dispersion and the variation of frequency with the oscilations of the amplitude.

The basic solutions of the equation are the plane waves, but the phase diagram is way more complex. It shows phase turbulence, defect turbulence, spirals, etc. [1] [2]. However, the CGLE is not known to support chimera states.

In this work, we will use variations over the general CGL equation, changing from the local interaction of the spatial derivative to non-local interactions with terms like:

$$\int G(x - x')A(x', t)dx'; \tag{1.2}$$

and look for chimera states in those variations.

1.2   Chimera States

A chimera state is defined as a spatio-temporal pattern in which a system of identical oscillators is split into coexisting regions of coherent (phase and frequency locked) and incoherent (drifting) oscillation [3]. On their own, neither of these behaviours were unexpected. Both incoherence and coherence were well documented in arrays of non-identical coupled oscillators, but complete incoherence and partial coherence were usually stable at different coupling strengths. This coexistence was found easily in systems with a frequency distribution [5]. However, this is not trivial to be formed in homogeneous systems. What makes the chimera states interesting is the possibility of finding in such a system a stable state in which both the coherent and the incoherent regimes coexist.

They take the name from the Greek mythology, where the chimera was a fire-breathing hybrid creature composed of the parts of more than one animal. Now the word refers to anything composed of incongrous parts.

Chimera states have been found in many discrete models, such as networks of oscillators or neurons [7], and there are even experimental results in the search of chimeras [4]. Nevertheless, chimera states in continuous systems are quite more elusive. There are some publications about chimera states found in continuous systems, but the conditions in which they have been found are the motivation of this work. In the next section, we will discuss the chimera states that have been found in the CGL equation using a non-local coupling.
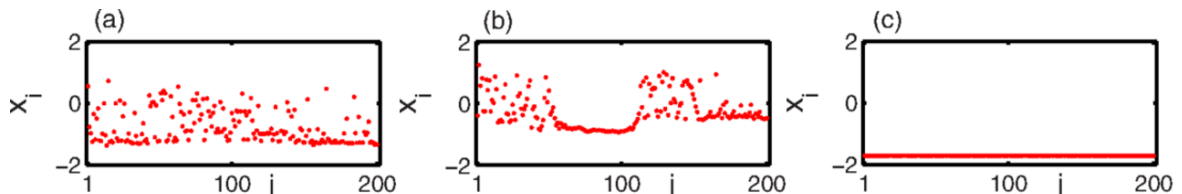

Figure 1.1: Example of a chimera state in a network of bursting neurons. The figure show the membrane potential x_i for each neuron i for the cases of incoherent regime (a), a coherent regime (c), and a chimera state (b), where both regimes coexist. The images have been taken directly from [7].

Chapter 2

The problem

In 2002, Y. Kuramoto and D. Battogtokh published a paper called "Coexistence of Coherence and Incoherence in Nonlocally Coupled Phase Oscillators[6]. In this paper, they proposed a continuous model based on the CGL equation, consisting in adding a nonlocal interaction to the equation; and in that model they found chimera states using numerical simulations. Nevertheless, a closer analysis of the results offered in the paper shows that there is something out of place.
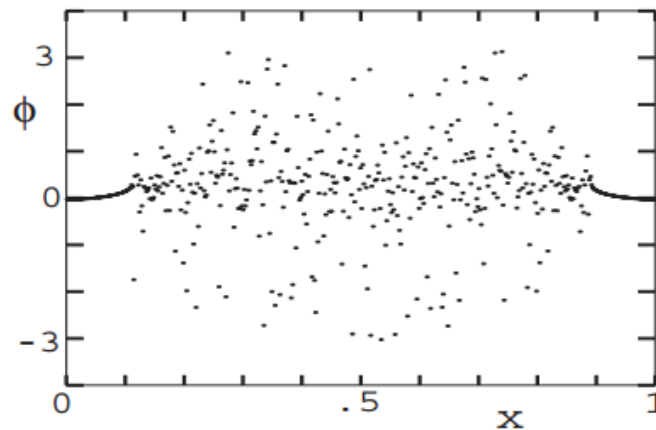

Figure 2.1: Chimera state found by Kuramoto and Battogtokh. The figure represents the argument of the field $\phi(x)$ as a function of the space, for the non-local CGLE in a periodic environment. The chimera is formed with the coexistence of the incoherent regime in the center of the figure with the coherent regime, located in the borders. In the incoherent regime, we can see the high discontinuities of the simulation. The figure has been taken directly from [6].

The results of the simulation shown in the paper do not represent a continuous system properly, as there is too much vertical distance between neighboring points (Figure 2.1 shows the result obtained in the paper). More technically, the simulations has aliasing, as the highest modes of the fourier transform of the simulations have non negligible amplitudes within the numerical precision, which in a numerical pseudo-spectral simulation is crucial for a good accuracy. In other words, fast spatial frequencies contributing to the dynamics are not resolved with enough precision.

Hence, the first step of this work is to reproduce these results, and analyze the Fourier transform of the simulation to confirm what, naked eyes, can be seen in the figures of Kuramoto and Battogtokh: that the simulation have aliasing, and therefore all the results may be spurious, caused by false interactions originated in the inaccuracies of the simulation.

2.1 Replica of the results

The proposed model is:

$$\frac{\partial}{\partial t}A(x,t) = (1 + i\omega_o)A - (1 + ib)|A|^2 A + K(1 + ia)\left(Z(x,t) - A(x,t)\right),\qquad (2.1)$$

where the function Z is the convolution product of the kernel G and the field:

$$Z(x,t) = \int G(x - x')A(x',t)dx'.\qquad (2.2)$$

In this particular case, the kernel used was an exponential:

$$G(y) = \frac{\kappa}{2}\exp(-\kappa|y|).\qquad (2.3)$$

Using a pseudo-spectral method to simulate the model proposed by Kuramoto Battogtokh [6], we could reproduce the results obtained by them in the paper with the same values of the parameteres. In the next figure, we can observe the chimera state and its Fourier transform:

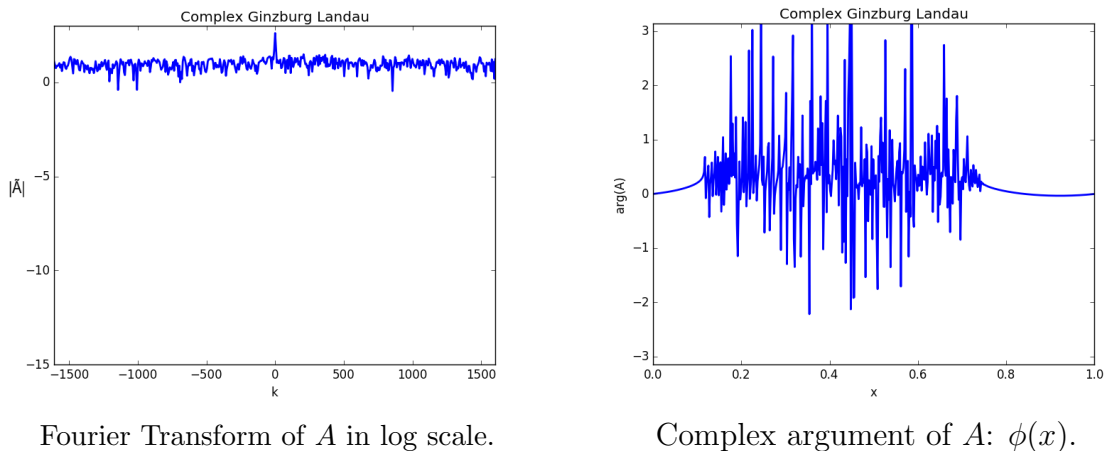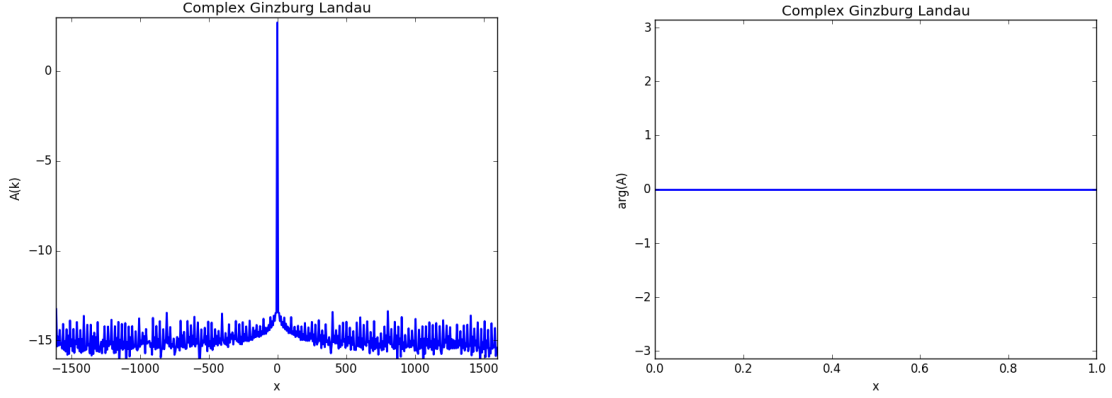Fourier Transform of A in log scale.   Complex argument of A: $\phi(x)$.

Figure 2.2: Replica of the chimeras obtained by [6] using our simulation of the non-local CGLE (equation 2.1). Parameters used: $N = 512$ (Number of points), $L = 1$ (system size), $\delta t = 0.05$, $\omega_0 = 1$, $b = 0.88$, $K = 0.1$, $\kappa = 4$ and $a = -1$.

A we can see, the Fourier components with the largest k have a large amplitude, much above the numerical precision. In a good simulation, higher frequencies in the Fourier transform should decay to the numerical precision, which is of the order of 10^{-15} for the amplitude of the Fourier transform. In the following figures (2.3-2.5), we show an

Fourier Transform of A in log scale.

Phase of A: ϕ.

Figure 2.3: Example of a correct simulation, for a plane wave solution of wave number $Q = 0$. Same parameters as in Fig. 2.2, but with $b = 0.6$.
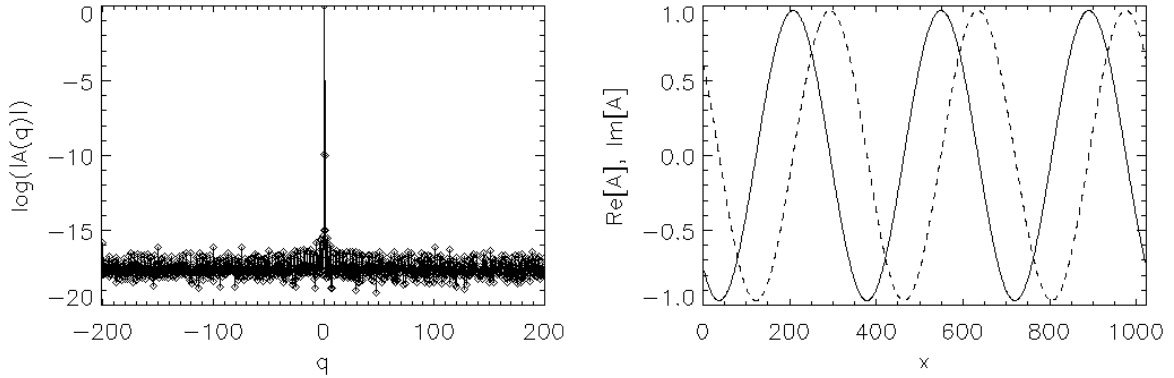

Figure 2.4: Example of a correct simulation, for a plane wave solution. Left: amplitude of the fourier transform in log scale. Right: Real and Imaginary (dashed line) parts of the field. Same parameters as in Fig. 2.3, but with $N = 1024$, $L = 64$ and $\kappa = 2$.

example of the equation solved correctly with precision for plane wave solutions and for the turbulent regime:

Therefore, the simulations showed in this work show that the chimera states reported by Kuramoto and Battogtokh [6] do not correspond strictly to a smooth numerical integration of the continuous system (the non local CGLE) that the authors intended to study, and stem from numerical artifacts (terms with large k above the numerical precision) in their numerical study of the equation. In this work, we intend to study the parameter space of the non local CGLE in search of chimera states.
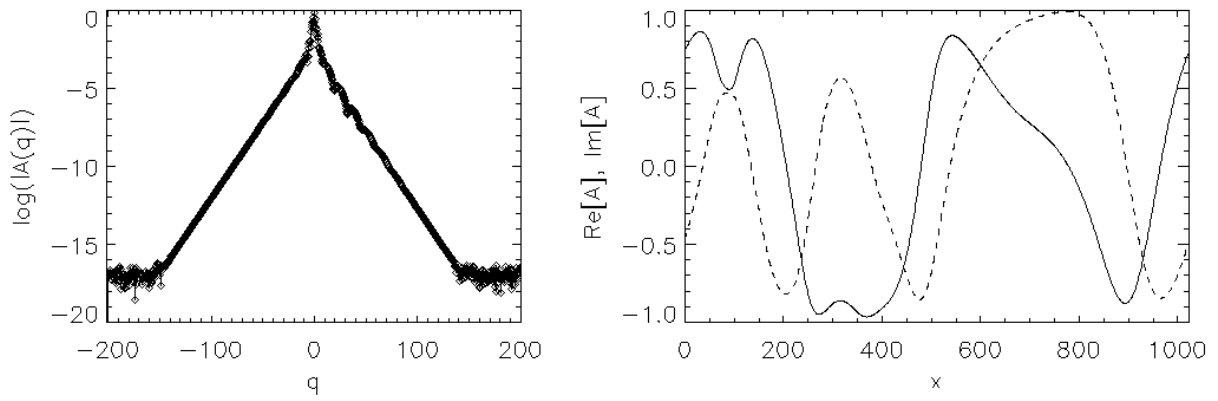
7

Figure 2.5: Example of a correct simulation in the turbulent regime. Left: amplitude of the fourier transform in log scale. Right: Real and Imaginary (dashed line) parts of the field. Same parameters as in Fig. 2.4, but with $b = 1.115$.

8

Chapter 3

Results

After proving that the simulations in Kuramoto and Battogtokh's paper were incorrect, the next step of this work is to make proper and precise simulations of the equations and find if proper chimera states exist in a well resolved numerical simulation.

As a starting point, we will look for chimera states in the model proposed in the paper, the CGL equation with an exponential kernel for a non-local interaction:

$$\frac{\partial}{\partial t}A = (\alpha_1 + i\alpha_2)A - (\beta_1 + i\beta 2)|A|^2 A + K(\gamma_1 + i\gamma_2)\left(Z(x,t) - A(x,t)\right), \qquad (3.1)$$

$$Z(x,t) = \int G(x - x')A(x',t)dx'. \qquad (3.2)$$

After studying this particular model, we can study more general variations using a different kernel or other non-linear terms.

3.1 Non-Local CGL with Exponential Kernel

In order to look for chimera states in the CGL with non-local interaction with exponential kernel, the first thing we made was to find analitically the stability of the plane wave solutions.

We propose a plane wave solution of the form:

$$A_0 = Fe^{i(Qx - wt + \phi)}, \qquad (3.3)$$

where:

$$|F|^2 = \frac{\alpha_1 - K\gamma_1\frac{Q^2}{\kappa^2 + Q^2}}{\beta_1} \qquad (3.4)$$

and

$$w = -\alpha_2 + \beta_2 F^2 + K\gamma_2 \frac{Q^2}{\kappa^2 + Q^2}. \tag{3.5}$$

Then, we apply a perturbation δa to this solution with the form:

$$A = \left[F + \delta a_+ e^{\lambda t + ikx} + \delta a_- e^{\lambda^* t - ikx} \right] e^{i(Qx - wt)} \tag{3.6}$$

By substitution, we can operate to find an expression for the value of λ, which is the growth rate of the perturbations. After all the calculations, we find two solutions: λ_+ and λ_-. As λ_- is always negative, we will focus in λ_+, which we will call λ. The complete calculations can be found in the appendix.

Using the analytical solution, we can find the transition from stability to instability of the plane wave solutions. In the following figure we plot the growth rate λ for different values of the control parameter β_2 close to that transition:

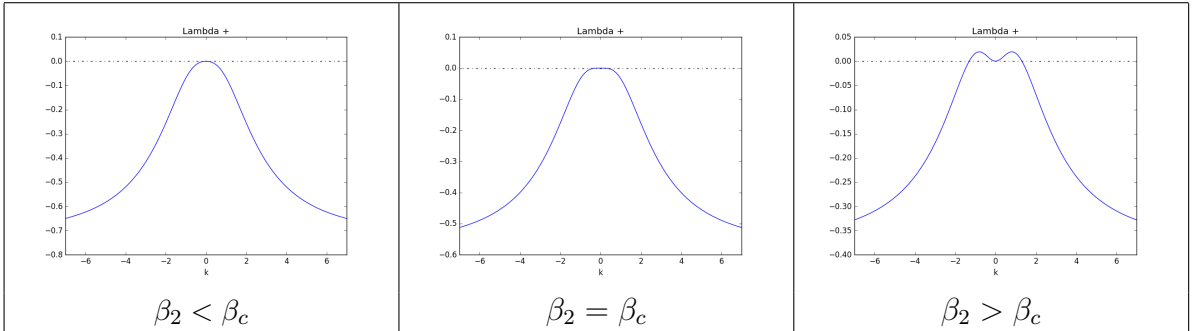| $\beta_2 < \beta_c$ | $\beta_2 = \beta_c$ | $\beta_2 > \beta_c$ |

Figure 3.1: Growth rate $\lambda_+(k)$ of the perturbations to the plane wave solution $Q = 0$ in the CGL with exponential kernel close to β_c. Parameters: $N = 512$, $L = 16$, $\alpha_1 = 1$, $\alpha_2 = 0$, $\beta_1 = 1$, $\kappa = 2$, $K = 1$, $\gamma_1 = 1$, $\gamma_2 = -1$. The value of β_c for this set of parameters is $\beta_c = 1$.

Plane wave solutions with higher wave number become unstable earlier increasing β. Therefore, the last stable one is the plane wave with $Q = 0$. The instability of the last plane wave signals the threshold for the so called Benjamin-Fair (BF) instability. Due to the form of the growth rate, we can make a Taylor expansion around 0:

$$\lambda = \lambda_0 + \lambda_1 k + \lambda_2 k^2 + O(k^3) \tag{3.7}$$

Finding the zeros in the coefficient λ_2, we can find the critical value of the parameters. In particular, we use β_2 as the control parameter. Figure 2.2 shows $\lambda_2(k)$ and the computed values for β_c.

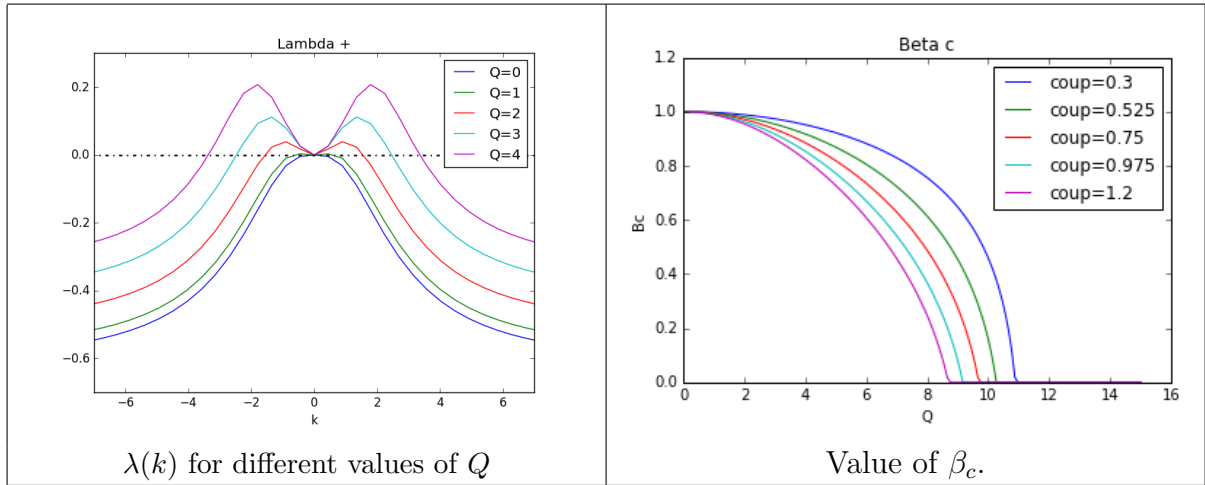$\lambda(k)$ for different values of Q Value of β_c.

Figure 3.2: Critical value of β_c depending on the wave number and the coupling strength labeled *coup* in the figure. Same parameters as in Fig. 3.1, but with $N = 2048$.

Figure 3.3 shows the stability region in parameter space of plane wave solutions with two different wave numbers. When $Q > 0$, the region of stability for the plane waves decreases with the coupling strength and even disappears for large values of the coupling strenght.

Stability of p.w. sol. with $Q = 0$ Stability of p.w. sol. with $Q = 1$
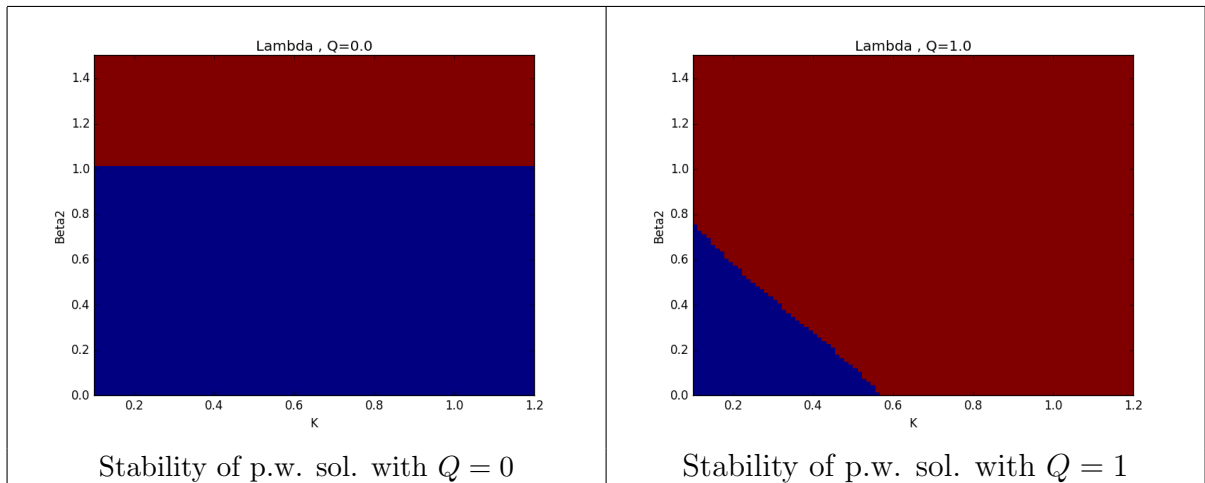
Figure 3.3: Stability diagram of plane wave solutions depending on the parameter β_2 and the coupling strength K. Red: Unstable, Blue: Stable. Same parameters as in Fig. 3.1, but with $K = 0.8$.

Once we have this information, we can start running simulations. After checking that the stability diagram agrees with the results of the simulations, we can start looking at the transition to see if there is any coexistence.

To characterize the transition to turbulence, we define an order parameter for the turbulence: the inverse of the slope of the Fourier transform in log scale "m":

$$\tilde{A}(k) \simeq Ce^{-pk}$$
$$m = 1/p \qquad (3.8)$$

We measured this order parameter in the simulation, and found that the transition is supercritical, as shown in Fiigure 3.5. In Figure 3.4 we can see an example of the simulation in the turbulent regime, where the Fourier transform displays the profile from which we have measured the slope to compute the order parameter.
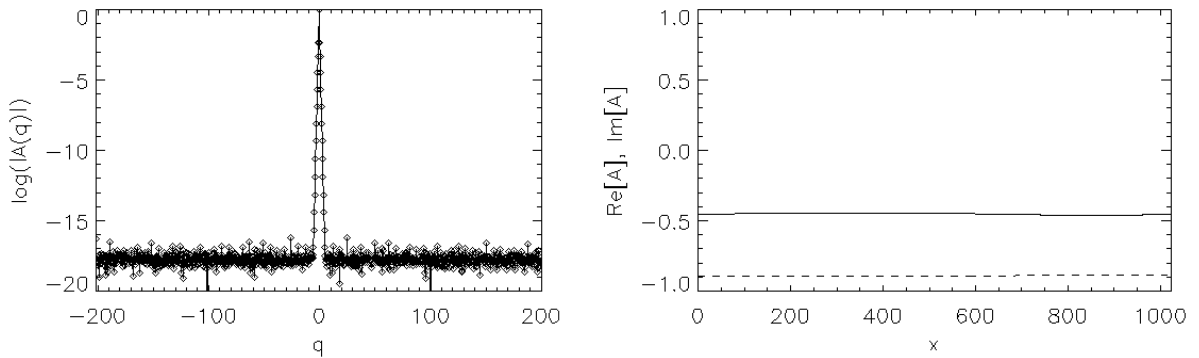
Figure 3.4: Simulation in the turbulent regime close to the bifurcation. Left: amplitude of the fourier transform in log scale. Right: Real and Imaginary (dashed line) parts of the field. From the slope in the fourier transform, we get the order parameter. Same parameters as in Fig. 2.5, but with $b = 1.01$.

We found that chimeras, in the equation proposed by Kuramotto B. [6] do not exist. The transition from the plane wave solution (coherent state) to the turbulence regime (incoherent state) is supercritical. Therefore, there is no room for a coexistence of both solutions, as only one of them is stable at each time.

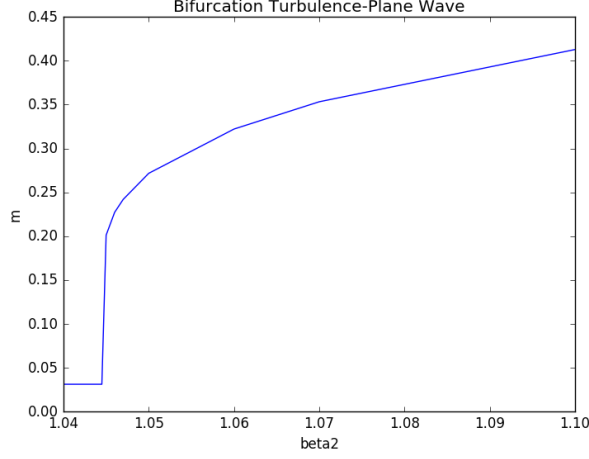Figure 3.5: Order parameter during the supercritical bifurcation in the transition from the plane wave solution to the turbulent regime obtained from the simulations. Same parameters as in Fig. 2.5.

3.2 Moment expansion for the kernel

We have shown that chimeras do not exist if we use an exponential kernel, but we could have used any other kernel. In order to make our study as general as possible, we will use a moment expansion of the kernel, which allows us to generalize the results to kernels that can be approximated with an expansion of even powers of the spatial derivatives:

$$Z(x,t) = \int G(x-x')A(x',t)dx' \simeq M_0 A + M_2 \partial_x^2 A + M_4 \partial_x^4 A + ... \tag{3.9}$$

If the kernel is normalized, then $M_0 = 1$. The equation now is:

$$\partial_t A = \alpha A - \beta |A|^2 A + \Gamma(M_2 \partial_x^2 A + M_4 \partial_x^4 A), \tag{3.10}$$

where we have contracted the complex parameters. The values used are:

$$\alpha = \alpha_1 + i\alpha_2 = 1, \qquad \beta = \beta_1 + i\beta_2 = 1 + i\beta_2, \\ \Gamma = \Gamma_1 + i\Gamma_2 = K(\gamma_1 + i\gamma_2) = K(1 - i). \tag{3.11}$$

This equation also has a plane wave solution:

$$A_0 = Fe^{i(Qx - \omega t + \phi)}, \tag{3.12}$$

where, in this case, we have these values for the amplitude and frequency:

$$|F|^2 = \frac{\alpha_1 + \Gamma_1(-M_2 Q^2 + M_4 Q^4)}{\beta_1}, \\ \omega = -\alpha_2 + \beta_2 |F|^2 + \Gamma_2 M_2 Q^2 - \Gamma_2 M_4 Q^4. \tag{3.13}$$

13

To analize the stability of the plane wave solution, we add a perturbation:

$$A = \left[F + \delta a_+ e^{\lambda t + ikx} + \delta a_- e^{\lambda^* t - ikx} \right] e^{i(Qx - wt)}. \tag{3.14}$$

Then, by substitution in the equation, we can operate in a similar way as the previous case (the exponential kernel) to obtain the solutions for the growth rate λ. The results obtained in this case are more complex, as we have 2 new parameters: M_2 and M_4. Using the analytical result for the growth rate, we can plot a diagram showing the regions for which the plane wave solutions are stable or unstable depending on the higher value of $\lambda(k)$ for each set of parameters (if there is any positive value, plane wave solutions are unstable).

The following figure shows the results obtained for the stability diagram. We also plot the growth rate for each of the quadrants:
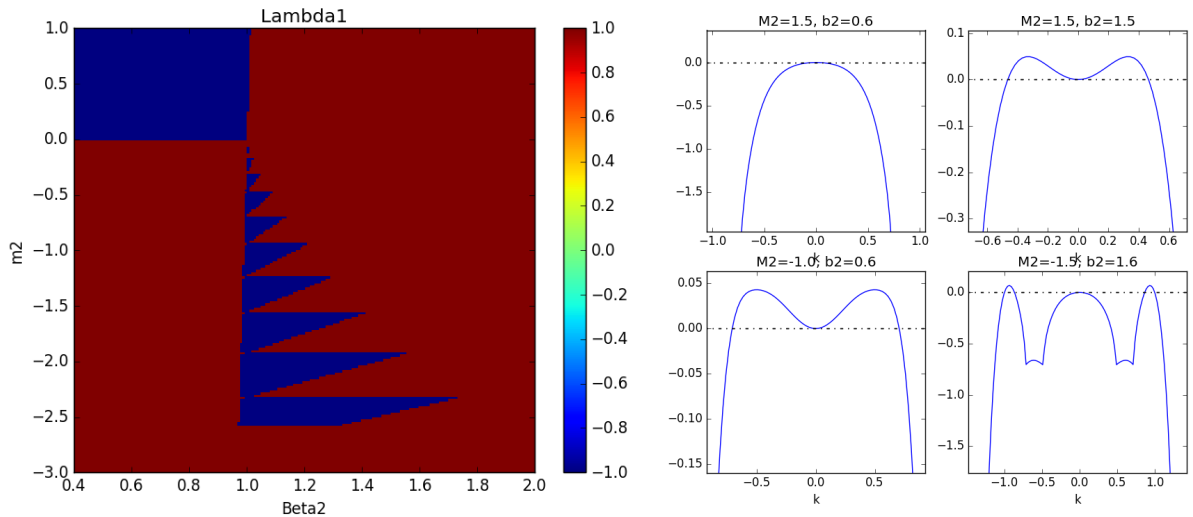
Figure 3.6: Left: Stability diagram for the CGL with Moment expansion of the kernel, for plane wave solutions with $Q = 0$. Red: Unstable. Blue: Stable. Right: Growth rate for different values of the parameters in the different quadrants. Parameters used: $N = 2048$, $L = 64$, $M_4 = -2$ and $K = 1.2$.

Using this diagram as a guide, we ran simulations of the equation in the transitions from stability to instability and viceversa. The transitions show a similar behavior to the equation with the exponential kernel: after crossing the analytical line of the transition, the behavior changes from plane wave to turbulence, or viceversa, without any coexistence as only one of the solutions is stable at each time. In the fourth quadrant we also have a new case, where the solution shows pattern formation, but the transition is still

supercritical.

In Figure 3.7 and Figure 3.8 we can see some examples of the simulation in the turbulent regime, and in the pattern formation regime. The figures show the amplitude of the Fourier transform in log-scale (top-left), the modulus of the field $|A|$ (top-right), the complex argument (bottom-left) and the real and imaginary parts of the field (bottom-right).

Figure 3.7: Simulation in the turbulent regime. Top left: amplitude of the Fourier Transform in log scale. Top right: $|A|$. Bottom left: complex argument of A. Bottom right: real and imaginary (dashed line) parts of A. Parameters used: $N = 512$, $L = 64$, $\beta_2 = 0.6$, $M_2 = -1$ and $M_4 = -2$.
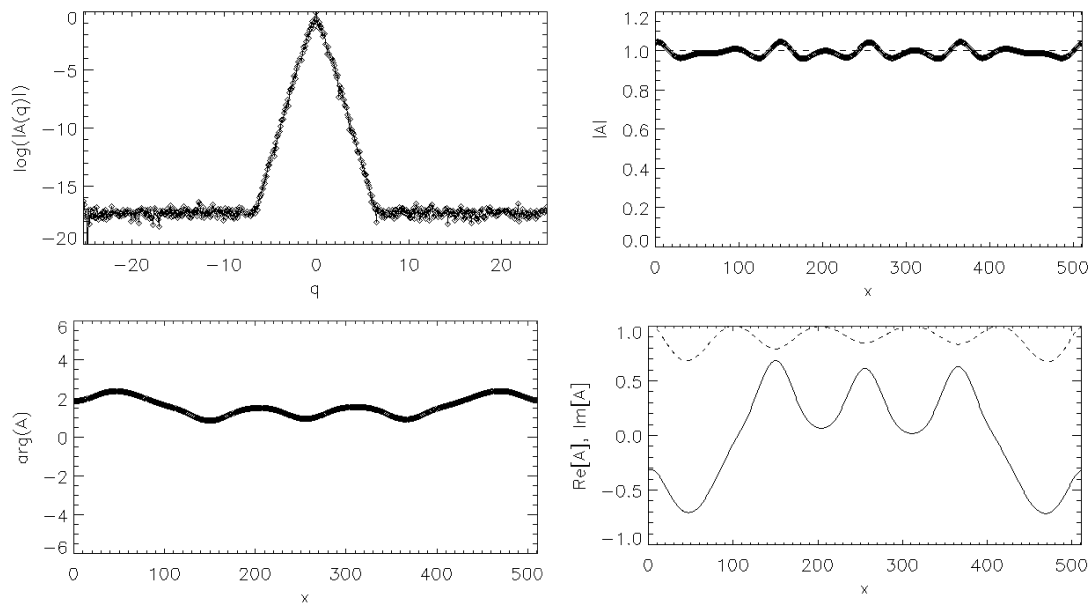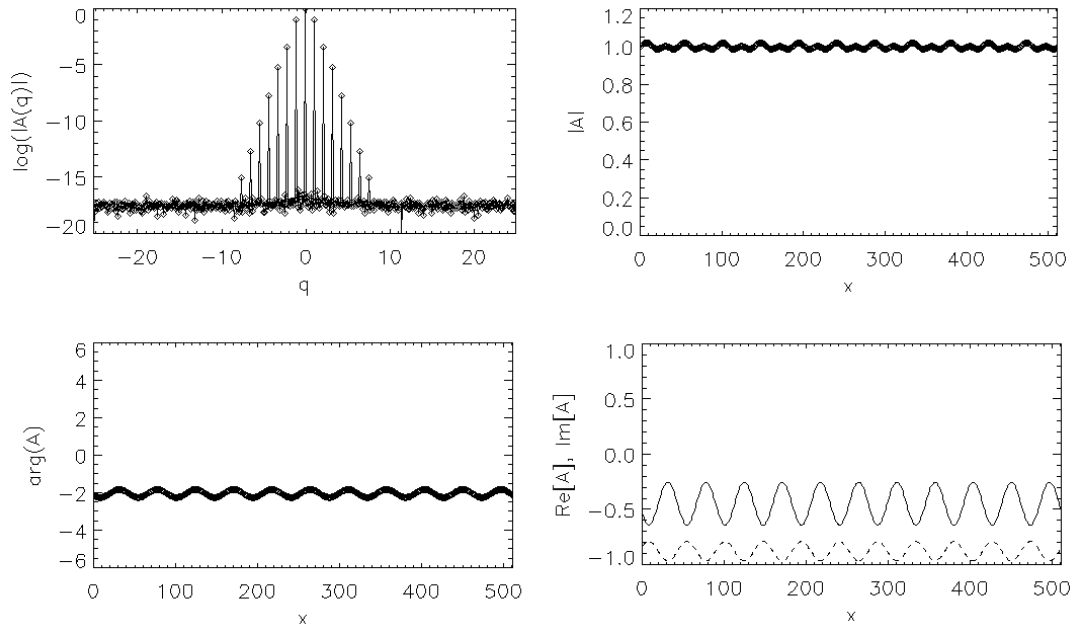
Figure 3.8: Simulation in the pattern formation regime. Top left: amplitude of the Fourier Transform in log scale. Top right: $|A|$. Bottom left: complex argument of A. Bottom right: real and imaginary (dashed line) parts of A. Same parameters as in Fig. 3.7, but with $\beta_2 = 1.6$ and $M_2 = -1.5$.

3.3 Moment expansion and Cubic-Quintic terms.

The next variation that we can introduce to the equation is another non-linear term. We are going to add a quintic term to the equation. We are also keeping the moment expansion for the kernel. The equation is left as follows:

$$\partial_t A = \alpha A + \beta|A|^2 A - c|A|^4 A + \Gamma(M_2\partial_x^2 + M_4\partial_x^4)A \tag{3.15}$$

where α, β, c and Γ are complex parameters.
This equations has plane wave solutions:

$$A_0 = Fe^{i(Qx-wt+\phi)} \tag{3.16}$$

$$|F_\pm|^2 = \frac{-\beta_1 \pm \sqrt{\beta_1^2 + 4c_1(\alpha_1 + \Gamma_1(-Q^2 M_2 + Q^4 M_4))}}{-2c_1}$$
$$\omega = -\alpha_2 - \beta_2|F|^2 + c_2|F|^4 - \Gamma_2(-Q^2 M_2 + Q^4 M_4) \tag{3.17}$$

To analize the stability of the plane wave solution, we add a perturbation:

$$A = \left[F + \delta a_+ e^{\lambda t + ikx} + \delta a_- e^{\lambda^* t - ikx}\right] e^{i(Qx-wt)}. \tag{3.18}$$

And study the growth rate λ, using a similar analysis as the used in the previous cases.[1] The stability diagram obtained from λ is shown in Figure 3.9.
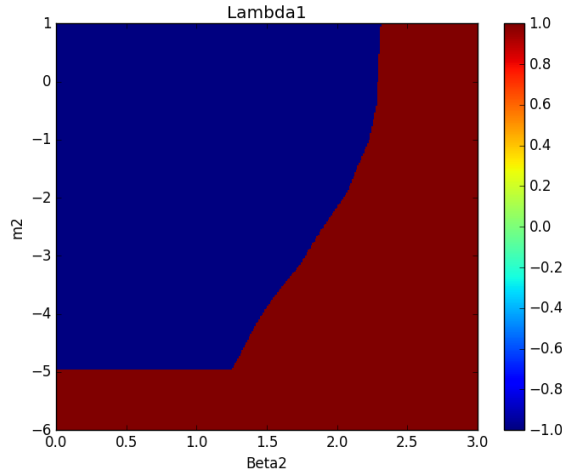

Figure 3.9: Stability of plane wave solutions (Blue: stable, Red: unstable). Parameters used: $N = 2048$, $L = 32$, $M_4 = -2$, $\alpha_1 = 1$, $\alpha_2 = 0$, $\beta_1 = 1$, $\gamma_1 = 1$, $\gamma_2 = -1$, $c_1 = 1$, $c_2 = -1$ and $K = 1.2$.

---

[1]The complete calculations can be found in the appendix.

By running simulations, we find that the transitions between the stable and unstable regime were similar as in the previous cases. The system was either in a plane wave state or in a turbulent state for each set of parameters, without observing any coexistence. Therefore, the existence of chimera states in this variation of the CGLE is also discarded.

A snapshot of the simulation in the turbulent regime is shown in Figure 3.10 . A similar order parameter as the one used in the first section of this chapter could be used to analyze the transition between the plane wave and the turbulent regimes.
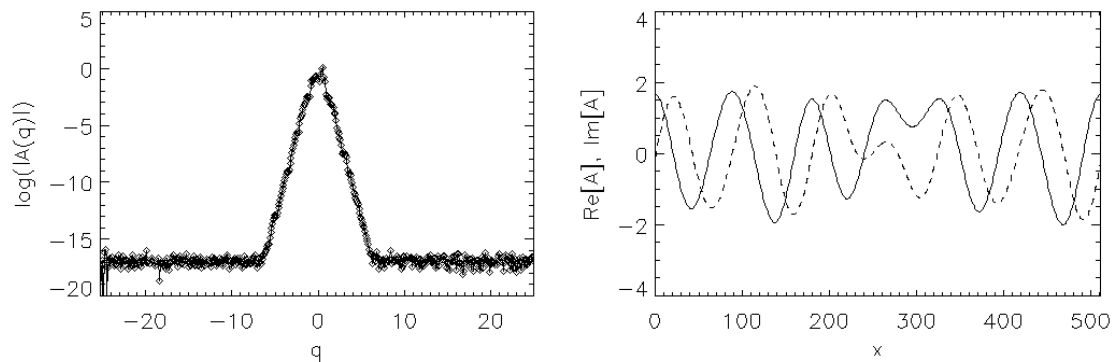

Figure 3.10: Simulation in the turbulent regime. Left: amplitude of the Fourier Transform of A. Right: real and imaginary (dashed line) parts of the field. Same parameters as in Fig. 3.9, but with $N = 512$, $\beta_2 = 2.3$ and $M_2 = -2$.

Chapter 4

Conclusions

We have found that the quimera states obtained by Kuramoto et al. were the product of computational errors, and therefore a spurious result of incorrect calculations. After doing proper simulations, we have found that chimera states do not exist in the model of the CGL with non-local interaction proposed by Kuramoto. We have found that the transition between the coherent (plane waves) and incoherent (turbulence) regimes was supercritical, leaving no possibility for a chimera state to develop in the transition.

Furthermore, we extended the study to others variations of the model, trying to find a condition for the chimera states to appear. First, we generalized the kernel using a moment expansion. From the study of the stability of the plane wave solutions and the transitions from stability and instability of those solutions, we have also found that there are no chimera states in the CGL equation with non-local coupling, independently of the kernel used.

Then, we have made a further step by studying the case of a cubic-quintic nonlinearity, but, with a similar analysis, we have found that we need some other ingredient in the equation in order to find chimera states in the CGL.

In summary, we have found that chimera states do not exist in the CGL equation with non-local coupling in 1D, and the results obtained by Kuramoto and Battogtokh [6] were not correct for a continuous system. As we have not found chimera states in any of the variations of the equation that we studied, we have concluded that a further study has to be made in order to find which kind of terms make the chimera states stable in the CGL equations in 1D.

Appendix A

Analysis of the stability of plane wave solutions.

A.1 Stability of Plane Wave Solutions in the non-local CGLE with Exponential Kernel

The CGL equation with the non-local interaction is:

$$\partial_t A = (\alpha_1 + i\alpha_2)A - (\beta_1 + i\beta_2)|A|^2 A + K(\gamma_1 + i\gamma_2)(Z - A) \tag{A.1}$$

where Z is the non-local interaction with the kernel G:

$$\begin{array}{c} Z = \int G(x - x')A(x', t)dx' \\ G(x) = \frac{\kappa}{2}e^{-\kappa|x|} \end{array} \tag{A.2}$$

This equation has plane wave solutions:

$$A_0 = Fe^{i(Qx - wt + \phi)} \tag{A.3}$$

$$\begin{array}{c} |F|^2 = \dfrac{\alpha_1 - K\gamma_1 \frac{Q^2}{\kappa^2 + Q^2}}{\beta_1} \\ w = -\alpha_2 + \beta_2 F^2 + K\gamma_2 \frac{Q^2}{\kappa^2 + Q^2} \end{array} \tag{A.4}$$

To study the stability of the plane wave solution, we add a perturbation:

$$A = \left[F + \delta a_+ e^{\lambda t + ikx} + \delta a_- e^{\lambda^* t - ikx} \right] e^{i(Qx - wt)} \tag{A.5}$$

We introduce the perturbation in the CGL equation. Let us study each term of the equation, starting with the temporal derivative:

$$\partial_t A = -iwA + e^{i(Qx - wt)} \left[\lambda \delta a_+ e^{\lambda t + ikx} + \lambda^* \delta a_- e^{\lambda^* t - ikx} \right]$$

20

Now, $|A|^2$:

$$|A|^2 = AA^* = |F|^2 + \delta a_+ F^* e^{\lambda t + ikr} + \delta a_- F^* e^{\lambda^* t - ikr} + F \delta a_+^* e^{\lambda^* t - ikr} + F \delta a_-^* e^{\lambda t + ikr} + O(\delta^2)$$

$$|A|^2 A = \begin{aligned} & e^{i(Qx - wt)} \left[|F|^2 F + \delta a_+^* F^2 e^{\lambda^* t - ikx} + \delta a_-^* F^2 e^{\lambda t + ikx} \right] + \\ & + e^{i(Qx - wt)} \left[2\delta a_+ |F|^2 e^{\lambda t + ikx} + 2\delta a_- |F|^2 e^{\lambda^* t - ikx} \right] + O(\delta^2) \end{aligned}$$

For the non-local interaction:

$$Z = \int G(x - x') A(x', t) dx' = \int dx' \frac{\kappa}{2} e^{-\kappa |x - x'|} e^{i(Qx' - wt)} \left[F + \delta a_+ e^{\lambda t + ikx} + \delta a_- e^{\lambda^* t - ikx'} \right] =$$

we split the integral for the two different cases of the absolute value:

$$= \frac{\kappa}{2} \int_{-\infty}^{x} dx' e^{-\kappa(x - x') + i(Qx' - wt)} A(x', t) + \frac{\kappa}{2} \int_{x}^{\infty} dx' e^{+\kappa(x - x') + i(Qx' - wt)} A(x', t)$$

and expand the expression:

$$\frac{Z}{\kappa/2} = F \left(e^{-\kappa x - iwt} \int_{-\infty}^{x} dx' e^{\kappa x' + iQx'} + e^{\kappa x - iwt} \int_{x}^{\infty} dx' e^{-\kappa x' + iQx'} \right) +$$

$$+ \delta a_+ e^{\lambda t - iwt} \left(e^{-\kappa x} \int_{-\infty}^{x} dx' e^{\kappa x' + iQx' + ikx'} + e^{\kappa x} \int_{x}^{\infty} dx' e^{-\kappa x' + iQx' + ikx'} \right) +$$

$$+ \delta a_- e^{\lambda^* t - iwt} \left(e^{-\kappa x} \int_{-\infty}^{x} dx' e^{\kappa x' + iQx' - ikx'} + e^{\kappa x} \int_{x}^{\infty} dx' e^{-\kappa x' + iQx' - ikx'} \right) =$$

we integrate the exponentials:

$$= F e^{-\kappa x - iwt} \left[\frac{e^{x'(\kappa + iQ)}}{\kappa + iQ} \right]_{-\infty}^{x} + F e^{\kappa x - iwt} \left[\frac{e^{x'(-\kappa + iQ)}}{-\kappa + iQ} \right]_{x}^{\infty} +$$

$$+ \delta a_+ e^{\lambda t - iwt} e^{-\kappa x} \left[\frac{e^{x'(\kappa + iQ + ik)}}{\kappa + iQ + ik} \right]_{-\infty}^{x} + \delta a_+ e^{\lambda t - iwt} e^{\kappa x} \left[\frac{e^{x'(-\kappa + iQ + ik)}}{-\kappa + iQ + ik} \right]_{x}^{\infty} +$$

$$+ \delta a_- e^{\lambda^* t - iwt} e^{-\kappa x} \left[\frac{e^{x'(\kappa + iQ - ik)}}{\kappa + iQ - ik} \right]_{-\infty}^{x} + \delta a_- e^{\lambda^* t - iwt} e^{\kappa x} \left[\frac{e^{x'(-\kappa + iQ - ik)}}{-\kappa + iQ - ik} \right]_{x}^{\infty}$$

as κ is positive, the exponentials go to zero at $\pm\infty$:

$$= F e^{-iwt + iQx} \left[\frac{1}{\kappa + iQ} - \frac{1}{-\kappa + iQ} \right] +$$

$$+ \delta a_+ e^{iQx - iwt + \lambda t + ikx} \left[\frac{1}{\kappa + iQ + ik} - \frac{1}{-\kappa + iQ + ik} \right] +$$

$$+\delta a_- e^{iQx-iwt+\lambda^* t-ikx} \left[\frac{1}{\kappa + iQ - ik} - \frac{1}{-\kappa + iQ - ik} \right]$$

finally:

$$\frac{Z}{\kappa/2} = F\frac{2\kappa e^{iQx-iwt}}{\kappa^2 + Q^2} + \frac{2\kappa\delta a_+ e^{i(Q+k)x+\lambda t+iwt}}{\kappa^2 + (Q+k)^2} + \frac{2\kappa\delta a_- e^{i(Q-k)x+\lambda^* t-iwt}}{\kappa^2 + (Q-k)^2}$$

we can compute $Z - A$:

$$Z - A = e^{i(Qx-wt)} \left\{ -F\frac{Q^2}{\kappa^2 + Q^2} - \delta a_+ e^{\lambda t+ikx}\frac{(Q+k)^2}{\kappa^2 + (Q+k)^2} - \delta a_- e^{\lambda^* t-ikx}\frac{(Q-k)^2}{\kappa^2 + (Q-k)^2} \right\}$$

Now, we can add all the terms. To simplify notation:

$$\partial_t A = \alpha A - \beta|A|^2 A + \gamma(Z - A)$$

$$\alpha = \alpha_1 + i\alpha_2, \quad \beta = \beta_1 + i\beta_2, \quad \gamma = K(\gamma_1 + i\gamma_2)$$

We can simplify the exponential $e^{i(Qx-wt)}$, as it is in every term. If we also cancel the terms from the plane wave, which is a solution for the equation:

$$\partial_t A_0 = \alpha A_0 - \beta|A_0|^2 A_0 + \gamma(Z - A_0) \tag{A.6}$$

that let us with:

$$0 = \delta a_+ e^{\lambda t+ikx} \left(iw - \lambda + \alpha - \beta|F|^2 2 - \gamma\frac{(Q+k)^2}{\kappa^2 + (Q+k)^2} \right) - \beta\delta a_-^* e^{\lambda t+ikx} +$$

$$+\delta a_- e^{\lambda^* t-ikx} \left(iw - \lambda^* + \alpha - \beta|F|^2 2 - \gamma\frac{(Q-k)^2}{\kappa^2 + (Q-k)^2} \right) - \beta F^2 \delta a_+^* e^{\lambda^* t-ikx} + O(\delta^2)$$

Now, we split the equation in two new equations, one with the terms with factor $e^{\lambda t+ikx}$, and another one with the terms with the factor $e^{\lambda^* t-ikx}$, which are independent:

$$\lambda\delta a_+ = \delta a_+ \left(iw + \alpha - \beta|F|^2 2 - \gamma\frac{(Q+k)^2}{\kappa^2 + (Q+k)^2} \right) - \beta F^2 \delta a_-^*$$

$$\lambda^*\delta a_- = \delta a_- \left(iw + \alpha - \beta|F|^2 2 - \gamma\frac{(Q-k)^2}{\kappa^2 + (Q-k)^2} \right) - \beta F^2 \delta a_+^*$$

If we take the complex conjugate of the second equation

$$\lambda\delta a_-^* = \delta a_-^* \left(-iw + \alpha^* - \beta^*|F|^2 2 - \gamma^*\frac{(Q-k)^2}{\kappa^2 + (Q-k)^2} \right) - \beta^*(F^*)^2 \delta a_+$$

22

that let us with a system of equations which can be written as a matrix:

$$M = \begin{pmatrix} iw + \alpha - \beta|F|^2 2 - \gamma\frac{(Q+k)^2}{\kappa^2+(Q+k)^2} & -\beta F^2 \\ -\beta^*(F^*)^2 & -iw + \alpha^* - \beta^*|F|^2 2 - \gamma^*\frac{(Q-k)^2}{\kappa^2+(Q-k)^2} \end{pmatrix} \quad \text{(A.7)}$$

$$\lambda \begin{pmatrix} \delta a_+ \\ \delta a_-^* \end{pmatrix} = M \begin{pmatrix} \delta a_+ \\ \delta a_-^* \end{pmatrix} \quad \text{(A.8)}$$

Now, to find the solutions for the values of λ, we have to find the eigenvalues of that matrix, solving the equation:

$$\lambda^2 - \tau\lambda + \Delta = 0 \quad \text{(A.9)}$$

where τ is the trace of the matrix, and Δ the determinant:

$$\tau = \alpha + \alpha^* - 2(\beta + \beta^*)|F|^2 - \gamma\frac{(Q+k)^2}{\kappa^2 + (Q+k)^2} - \gamma^*\frac{(Q-k)^2}{\kappa^2 + (Q-k)^2} =$$

$$\tau = 2\alpha_1 - 4\beta_1|F|^2 - \gamma\frac{(Q+k)^2}{\kappa^2 + (Q+k)^2} - \gamma^*\frac{(Q-k)^2}{\kappa^2 + (Q-k)^2} \quad \text{(A.10)}$$

$$\Delta = \left(iw + \alpha - \beta|F|^2 2 - \gamma\frac{(Q+k)^2}{\kappa^2+(Q+k)^2}\right)\left(-iw + \alpha^* - \beta^*|F|^2 2 - \gamma^*\frac{(Q-k)^2}{\kappa^2+(Q-k)^2}\right) \\ -|\beta|^2|F|^4 \quad \text{(A.11)}$$

Therefore, the solutions for the growth rate λ are:

$$\lambda_\pm = \frac{\tau \pm \sqrt{\tau^2 - 4\Delta}}{2} \quad \text{(A.12)}$$

A.2 Stability of Plane Wave Solutions in the non-local CGLE with Moment expansion for the kernel.

The CGL equation with Moment expansion for the non-local interaction has the following expression:

$$\partial_t A = \alpha A - \beta |A|^2 A + \Gamma(M_2 \partial_x^2 + M_4 \partial_x^4)A \tag{A.13}$$

To find the plane wave solution,

$$A_0 = Fe^{i(Qx-\omega t)}, \tag{A.14}$$

we substitute in the equation and split real and imaginary parts:

$$\left.\begin{array}{ll} Real: & 0 = \alpha_1 - \beta_1|F|^2 - \Gamma_1 M_2 Q^2 + \Gamma_1 M_4 A_0 \\ Imag.: & \omega = \alpha_2 - \beta_2|F|^2 - \Gamma_2 M_2 Q^2 + \Gamma_2 M_4 Q^4 \end{array}\right\}$$

and we find:

$$\begin{array}{l} |F|^2 = \frac{\alpha_1 + \Gamma_1(-M_2 Q^2 + M_4 Q^4)}{\beta_1} \\ \omega = \alpha_2 - \beta_2|F|^2 - \Gamma_2 M_2 Q^2 + \Gamma_2 M_4 Q^4 \end{array} \tag{A.15}$$

To study the stability of this solution, we add a perturbation:

$$A = \left[F + \delta a_+ e^{\lambda t + ikx} + \delta a_- e^{\lambda^* t - ikx}\right] e^{i(Qx-wt)}, \tag{A.16}$$

and we introduce it in the CGL equation. For the temporal derivative and the cubic term, we have the same expression as in the previous case. For the spatial derivatives, we have:

$$\partial_x^2 A = \left\{-Q^2 F - \delta a_+(Q+k)^2 e^{\lambda t+ikx} - (Q-k)^2 \delta a_- e^{\lambda^* t-ikx}\right\} e^{i(Qx-\omega t)}$$

$$\partial_x^4 A = \left\{+Q^4 F + \delta a_+(Q+k)^4 e^{\lambda t+ikx} + (Q-k)^4 \delta a_- e^{\lambda^* t-ikx}\right\} e^{i(Qx-\omega t)}$$

If we sum all terms, and cancel the factor $e^{i(Qx-\omega t)}$ present in every term, we have:

$$\begin{aligned} 0 = \ & [(i\omega + \alpha)F - \beta|F|^2 F + \Gamma M_2(-Q^2)F + \Gamma M_4 Q^4 F] + \\ & + \delta a_+ \left[-\lambda + i\omega + \alpha - 2\beta|F|^2 - (Q+k)^2 \Gamma M_2 + (Q+k)^4 \Gamma M_4\right] e^{\lambda t+ikx} + \\ & + \delta a_- \left[-\lambda^* + i\omega + \alpha - 2\beta|F|^2 - (Q-k)^2 \Gamma M_2 + (Q-k)^4 \Gamma M_4\right] e^{\lambda^* t-ikx} + \\ & - \beta F^2 \delta a_+^* e^{\lambda^* t-ikx} - \beta F^2 \delta a_-^* e^{\lambda t+ikx} \end{aligned}$$

The first square bracket is equal to zero, as it is the plane wave solution. We can split the rest of the equation in 2, as $e^{\lambda t+ikx}$ is orthogonal to $e^{\lambda^* t-ikx}$:

$$
\begin{array}{ll}
e^{\lambda t + ikx}\big) & 0 = \delta a_+ \left[-\lambda + i\omega + \alpha - 2\beta |F|^2 - (Q+k)^2 \Gamma M_2 + (Q+k)^4 \Gamma M_4 \right] - \beta F^2 \delta a_-^* \\
e^{\lambda^* t - ikx}\big) & 0 = \delta a_- \left[-\lambda^* + i\omega + \alpha - 2\beta |F|^2 - (Q-k)^2 \Gamma M_2 + (Q-k)^4 \Gamma M_4 \right] - \beta F^2 \delta a_+^*
\end{array}
$$

Now, if we take the complex conjugate of the second equation, we can put the system in a matricial form:

$$
\lambda \begin{pmatrix} \delta a_+ \\ \delta a_-^* \end{pmatrix} = M \begin{pmatrix} \delta a_+ \\ \delta a_-^* \end{pmatrix}
\tag{A.17}
$$

where the matrix M is:

$$
M = \begin{pmatrix} M_{1,1} & -\beta F^2 \\ -\beta^* F^{*2} & M_{2,2} \end{pmatrix}
\tag{A.18}
$$

where:

$$
\begin{array}{l}
M_{1,1} = i\omega + \alpha - (Q+k)^2 \Gamma M_2 - 2\beta |F|^2 + (Q+k)^4 \Gamma M_4 \\
M_{2,2} = i\omega + \alpha - (Q-k)^2 \Gamma M_2 - 2\beta |F|^2 + (Q-k)^4 \Gamma M_4
\end{array}
\tag{A.19}
$$

We can solve this equation to find the values of λ from the eigenvalues of the matrix M:

$$
\lambda^2 - \tau \lambda + \Delta = 0
\tag{A.20}
$$

where τ and Δ are the trace and the determinant of M:

$$
\begin{array}{c}
\tau = 2\alpha_1 - 4|F|^2 \beta_1 - \Gamma M_2 (Q+k)^2 - \Gamma^* M_2 (Q-k)^2 + \Gamma M_4 (Q+k)^4 + \Gamma^* M_4^* (Q-k)^4 \\
\Delta = -|\beta|^2 |F|^4 + M_{1,1} M_{2,2}
\end{array}
\tag{A.21}
$$

We find that the solutions for λ are:

$$
\lambda_\pm = \frac{\lambda \pm \sqrt{\tau^2 - 4\Delta}}{2}
\tag{A.22}
$$

We can use the computer to plot this expression for each set of parameters, as a function of k.

A.3 Stability of Plane Wave Solutions in the CGL equation with Cubic-Quintic terms and Moment expansion for the kernel.

The equation in this case is:

$$\partial_t A = \alpha A + \beta |A|^2 A - c|A|^4 A + \Gamma(M_2 \partial_x^2 A + M_4 \partial_x^4 A), \tag{A.23}$$

where α, β, c and Γ are complex parameters. Again, we introduce the plane wave expression in the equation to find the solutions for the amplitude and frequency:

$$A_0 = Fe^{i(Qx-\omega t)} \tag{A.24}$$

$$|F|^2 = \frac{-\beta_1 \pm \sqrt{\beta_1^2 + 4c[\alpha_1 + \Gamma_1(-Q^2 M_2 + Q^4 M_4)]}}{-2c_1}$$
$$\omega = -\alpha_2 - \beta_2 |F|^2 + c_2 |F|^4 - \Gamma_2(-Q^2 M_2 + Q^4 M_4) \tag{A.25}$$

In this case, we have 2 different solutions for the amplitude of the plane waves. To find the stability, we add a perturbation to the plane wave of the form:

$$A = \left[F + \delta a_+ e^{\lambda t + ikx} + \delta a_- e^{\lambda^* t - ikx} \right] e^{i(Qx-wt)}, \tag{A.26}$$

We can introduce this expression in the equation to find the solutions for λ. The expansion of the quintic term is:

$$|A|^4 A = \left(|F|^4 F + \delta a_+ e_+ 3|F|^4 + \delta a_- e_- 3|F|^4 + \delta a_+^* e_- 2|F|^2 F^2 + \delta a_-^* e_+ 2|F|^2 F^2 \right) e_0 + O(\delta^2)$$

where:

$$e_0 = e^{i(Qx-\omega t)}, \qquad e_+ = e^{\lambda t + ikx}, \qquad e_- = e^{\lambda^* t - ikx}.$$

The rest of the terms have been analyzed in previous sections of the appendix. Now, we can make the sum:

$$\begin{aligned} 0 = \quad & [(i\omega + \alpha)F + \beta |F|^2 F - c|F|^4 F + F\Gamma(-Q^2 M_2 + Q^4 M_4)] + \\ & \delta a_+ e_+ [-\lambda + i\omega + \alpha + 2\beta |F|^2 - 3c|F|^4 + \Gamma(-(Q+k)^2 M_2 + (Q+k)^4 M_4)] + \\ & \delta a_- e_- [-\lambda^* + i\omega + \alpha + 2\beta |F|^2 - 3c|F|^4 + \Gamma(-(Q-k)^2 M_2 + (Q-k)^4 M_4)] + \\ & \delta a_+^* e_- [\beta F^2 - 2c|F|^2 F] + \delta a_-^* e_+ [\beta F^2 - 2c|F|^2 F^2] \end{aligned}$$

The first square bracket cancels, as it is the solution of the CGL equation. We can split the terms with e_+ and e_- in two different equations, as in the previous cases. Then, if we take the complex conjugate of the second equation, we can express that system in a matricial form:

$$\lambda \begin{pmatrix} \delta a_+ \\ \delta a_-^* \end{pmatrix} = M \begin{pmatrix} \delta a_+ \\ \delta a_-^* \end{pmatrix} \tag{A.27}$$

with the following matrix M:

$$M_{1,1} = i\omega + \alpha + 2\beta|F|^2 - 3c|F|^4 + \Gamma\left[(Q+k)^4 M_4 - (Q+k)^2 M_2\right]$$
$$M_{2,2} = -i\omega + \alpha^* + 2\beta^*|F|^2 - 3c^*|F|^4 + \Gamma^*\left[(Q-k)^4 M_4^* - (Q-k)^2 M_2^*\right] \qquad \text{(A.28)}$$
$$M_{1,2} = \beta F^2 - 2c|F|^2 F = M_{2,1}^*$$

We find the growth rate from the eigenvalues of the matrix M:

$$\lambda^2 - \tau\lambda + \Delta = 0, \qquad \text{(A.29)}$$

where τ is the trace of M and Δ its determinant:

$$\tau = 2\alpha_1 + 4|F|^2\beta_1 - 6c_1|F|^4 + \Gamma\left[-M_2(Q+k)^2 + M_4(Q+k)^4\right] + \Gamma^*\left[-M_2^*(Q-k)^2 + M_4^*(Q-k)^4\right]$$
$$\Delta = -\left|\beta F^2 - 2c|F|^2 F^2\right|^2 + M_{1,1}M_{2,2}$$

$$\text{(A.30)}$$

The final solution is:

$$\lambda_\pm = \frac{\tau \pm \sqrt{\tau^2 - 4\Delta}}{2} \qquad \text{(A.31)}$$

Appendix B

Numerical methods

The time evolution of the complex field A(x,t) subjected to periodic boundary conditions is obtained numerically from the integration of the CGL in Fourier space. The method, used as described by [9], is pseudospectral and second-order accurate in time. Each Fourier mode A_k evolves according to:

$$\delta_t A_k(t) = -\alpha_k A_k(t) + \Phi_k(t) \tag{B.1}$$

where α_k corresponds to the linear terms, and Φ_k is the amplitude of mode k of the nonlinear terms in the $CGLE$. The value of α has the following values for each of the cases studied in this work:[1]

$\partial_t A = \alpha A - \beta|A|^2 A + \Gamma(Z - A)$	$\alpha_k = \alpha + \Gamma(G_k - 1)$
$\partial_t A = \alpha A - \beta|A|^2 A + \Gamma(M_2 \partial_x^2 + M_4 \partial_x^4)A$	$\alpha_k = \alpha + \Gamma(-M_2 k^2 + M_4 k^4)$
$\partial_t A = \alpha A + \beta|A|^2 A - c|A|^4 A + \Gamma(M_2 \partial_x^2 A + M_4 \partial_x^4 A)$	$\alpha_k = \alpha + \Gamma(-M_2 k^2 + M_4 k^4)$

The amplitudes Φ_k are calculated, at any time, by taking the inverse Fourier transform $A(x, t)$ of A_k, computing the nonlinear term in real space, and then calculating the direct Fourier transform of this term. A standard fast Fourier transform subroutine is used for this purpose.

---

[1]

For the CGL with non local interactions and exponential kernel, if we go to Fourier space, Z is a convolution product, so we can write:
$$Z_k(t) = G_k A_k(t).$$
Therefore, for the linear part, we have:

$$\alpha_k = \alpha + \Gamma(G_k - 1).$$

Equation B.1 is integrated numerically in time by using a method similar to the so-called two-step method [10]. For convenience in the notation, the time step is defined here such that the time is increased by $2\delta t$ at each iteration.

When a large number of modes k are used, the linear time scales α_k can take a wide range of values. A way of circumventing this stiffness problem is to treat exactly the linear terms by using a formal solution

$$A_k(t) = e^{-\alpha_k t}\left(A_k(t_0)e^{\alpha_k t_0} + \int_{t_0}^{t} \Phi_k(s)e^{\alpha_k s}ds \right). \tag{B.2}$$

From this the following relationship is found:

$$\frac{A_k(t + \delta t)}{e^{-\alpha_k \delta t}} - \frac{A_k(t - \delta t)}{e^{\alpha_k \delta t}} = e^{-\alpha_k t}\int_{t-\delta t}^{t+\delta t} \Phi_k(s)e^{\alpha_k s}ds.$$

The taylor expansion of $\Phi_k(s)$ around $s = t$ for small δt gives an expression for the right-hand side:

$$\Phi_k(t)\frac{e^{\alpha_k \delta t} - e^{-\alpha_k \delta t}}{\alpha_k} + O(\delta t^3).$$

Substituting this result, we get:

$$A_k(n + 1) = e^{-2\alpha_k \delta t}A_k(n - 1) + \frac{1 - e^{-2\alpha_k \delta t}}{\alpha_k}\Phi_k(n) + O(\delta t^3), \tag{B.3}$$

where expressions of the form $f(n)$ are abbreviations for $f(t = n\delta t)$. Expression B.3 is the so-called salved leapfrog of Frisch et al. [11]. To use this scheme the values of the field at the first two time stems are required. Nevertheless, this scheme alone is unstable for the CGL. This is not explicitly stated in the literature and probably a corrective algorithm is also applied. Obtaining such a correction is straightforward: Following steps similar to the ones before, one derives the auxiliary expression:

$$A_k(n) = e^{-\alpha_k \delta t}A_k(n - 1) + \frac{1 - e^{-\alpha_k \delta t}}{\alpha_k}\Phi_k(n - 1) + O(\delta t^2). \tag{B.4}$$

The numerical method we use, which we will refer to as the two-step method [9], provides the time evolution of the field from a given initial condition by using Eqs. B.3 and B.4 as follows:

1. $\Phi_k(n - 1)$ is calculated from $A_k(n - 1)$ by going to real space,

2. Eq. B.4 is used to obtain an approximation to $A_k(n)$,

3. the nonlinear term $\Phi_k(n)$ is now calculated from this $A_k(n)$ by going to real space, and

4. the field at step $n+1$ is calculated from Eq. B.3 by using $A_k(n-1)$ and $\Phi_k(n)$.

At each iteration, we get $A_k(n+1)$ from $A_k(n-1)$ and the time advances by $2\delta t$. Note that the total error is $O(\delta t^3)$, despite that the error in the intermediate value obtained with Eq. B.4 is $O(\delta t^2)$.

The number of Fourier modes depends on the space discretization. We have used a system size of $L = 32$, with $dx = L/N$ and usually $N = 1024$ or $N = 2048$. The time step used was $dt = 2\delta t = 0.001$. The method has been tested by integrating plane wave solutions for each of the cases, as we have the analytical solution for the expected amplitude and frequency of the plane waves. A further analysis on the accuracy of the numerical method can be found in [9].

Bibliography

[1] H. Chaté, and P. Manneville, *Phase diagram of the two-dimensional complex Ginzburg-Landau equation.* , Physica A **224**, 348.(1996)

[2] I. S. Aranson and L. Kramer. *The world of the complex Ginzburg-Landau equation.* Rev. Mod. Phys. **74**, 99 (2002).

[3] D. M. Abrams, S. H. Strogatz. *Chimera states for coupled oscillators.* Phys Rev Lett. **93**, 174102 (2004).

[4] E. A. Martens, S. Thutupalli, A. Fourrière and O. Hallateschek. *Chimera states in mechanical oscillator networks.* Proceedings of the National Academy of Sciences of the United States of America **110**, 26 (2013).

[5] S. H. Strogatz. *From Kuramoto to Crawford: exploring the onset of synchronization in populations of coupled oscillators.* Physica D Nonlinear Phenomena **143**, 1 (2000).

[6] Y. Kuramoto and D. Battogtokh. *Coexistence of Coherence and Incoherence in Non-locally Coupled Phase Oscillators.* Nonlinear Phenomena in Complex Systems **5**, 380 (2002).

[7] B. K. Bera, D. Ghosh and M. Lakshmanan. *Chimera states in bursting neurons.* Physical Review E **93** (2015).

[8] M. J. Panaggio and D. M. Abrams. *Chimera states: coexistence of coherence and incoherece in networks of coupled oscillators.* London Mathematical Society, Nonlinearity **28**, 3 (2015).

[9] R. Montagne, E. Hernández-García, A. Amengual, M. San Miguel, *Wound-up phase turbulence in the complex Ginzburg-Landau equation.* Physical Review E **56**, 151 (1997).

[10] D. Potter, *The construction of discrete orthogonal coordinates*, Computational Physics, **13**, 483, (1973).

[11] U.Frisch, Z. S. She, and O. Thual, *Viscoelastic behaviour of cellular solutions to the Kuramoto-Sivashinsky model.* J. Fluid Mech. **168**, 221 (1986).